Fermi National Accelerator Laboratory

FERMILAB-Conf-95/346-E
CDF

B Physics Results at CDF

J.C. Yun
The CDF Collaboration

Fermi National Accelerator Laboratory
P.O. Box 500, Batavia, Illinois 60510

November 1995

Talk Given at the *3rd International Workshop on B Physics at Hadron Machines*, Oxford, UK, July 10-14, 1995

Operated by Universities Research Association Inc. under Contract No. DE-AC02-76CHO3000 with the United States Department of Energy

Disclaimer

FERMILAB-CONF-95/346-E
CDF/PUB/BOTTOM/PUBLIC/3370

B Physics Results at CDF [1]

the CDF Collaboration
J.C. Yun

Fermi National Accelerator Laboratory
Batavia, Illinois, USA

Abstract

In this paper we present B physics results from 1.8 Tev proton-antiproton collisions recorded with the Collider Detector at Fermilab(CDF). Measurements of the B meson masses, lifetimes, $B^o\bar{B}^o$ mixing, and polarization are described. The prospects for measuring CP violation with the upgraded Fermilab collider and CDF detector are also briefly described.

[1] Talk given at the 3rd International Workshop on B-Physics at Hadron Machines, Oxford, UK, 10-14 July, 1995.

1 Introduction

In $p\bar{p}$ collisions at high energy, b quarks are produced copiously. The measured b cross section at 1.8 TeV center of mass energy in the pseudorapidity region $|\eta| \leq 1.0$ is about $30\mu b$[1]. At the typical Tevatron luminosity of $\sim 10^{31} cm^{-2} sec^{-1}$, about 300 $b\bar{b}$ events are produced every second. Handling the background events which are 1000 times more frequent is the most critical part of the trigger system at CDF. Since most of b quarks are produced at very low p_t region (most probable p_t $\sim$2 GeV/c), it is a challenging task to trigger efficiently. In CDF, leptons are the major source of triggers for b events. Low p_t b events are accessible using the clean signature of their leptonic decays. Successful implementation of lepton triggers has enabled CDF to join the arena of highly competitive b physics.

The data described in this paper were taken during the 1992-1995 runs using the CDF detector. Most of the results presented in the paper are from RUN 1A (1992-1993) data with an integrated luminosity of 20 pb^{-1} while a few results include RUN 1B (1994-1995) data with an integrated luminosity of $\sim$50 pb^{-1} . In the following, we present results of b meson masses, lifetimes, $B^o\bar{B}^o$ mixing, polarization, and the prospects for a CP violation measurement with the RUN II (1999) data.

1.1 CDF Detector

The CDF detector has been described in detail elsewhere [2]. We briefly describe the subsystems which are important for the analysis. The silicon vertex chamber (SVX) [3] consists of four layers of silicon detectors located between 2.9 and 7.9 cm in radius and extends $\pm$25cm in z from the center of the interaction region. It provides spatial measurements for the charged tracks with an impact parameter resolution of $\sim$13 μm in the $r\phi$ plane. The geometric acceptance of the SVX is $\sim$60% as the z interaction distribution has a Gaussian like shape with σ of $\sim$30cm. Surrounding the SVX is a time projection chamber (VTX) which provides tracking measurement in r-z plane. Momenta of charged particles are measured by a large volume cylindrical drift chamber, the central tracking chamber(CTC), which has an accuracy of $\Delta p_t/p_t = [(0.0009 \cdot p_t)^2 + (0.0066)^2]^{1/2}$. The CTC covers the pseudorapidity range $|\eta| \leq 1.1$, where $\eta = -ln[tan(\theta/2)]$. These tracking chambers are inside of a superconducting solenoid which provides a 1.4 Tesla axial magnetic field. Electromagnetic and hadronic calorimeters are located outside the solenoid.

1.2 Lepton Identification

The central muon system, CMU, covers $|\eta| \leq 0.6$ behind 4 interaction lengths of material which are provided by the central calorimeters. The central muon upgrade, CMP, are located behind the CMU and covers the same η region with an additional filter of 60 cm thick steel for reduction of the backgrounds. The central muon extension, CMX, covers $0.6 \leq |\eta| \leq 1.0$ with absorption material provided by the central calorimeters. The p_t thresholds for the lepton triggers are constrained by the background rate and data logging capability. The inclusive muon trigger p_t threshold is set to be $\geq$8 GeV/c .

The low p_t electrons are identified in the central calorimeters. At the trigger level, an electron is required to have an electromagnetic shower and a trigger track match. The inclusive electron trigger p_t threshold is set to be $\geq$8 GeV/c . For dilepton triggers, the p_t thresholds are further reduced to accept low p_t b events. For $\mu\mu$ the particle p_t thresholds are 2 GeV/c and for $e\mu$ they are 5 GeV/c and 3 GeV/c , respectively.

2 B Meson Mass Measurement

In CDF $\sim$20 % of J/ψ and ψ' samples are from $b\bar{b}$ events. Unlike other lepton samples these samples do not have missing neutrinos; hence full reconstruction of B mesons is possible. First, $J/\psi \to \mu^+\mu^-$ events are selected from the dimuon trigger. The muon selection criterion is a three dimensional CTC track pointing to a muon track in one of the three muon chambers. The matching requirement is 3σ, where σ is the matching uncertainty between the CTC track and the muon track. If the CTC track matches with SVX hits, the combined track information is used. The invariant mass of the pair of oppositely charged muons is required to be within 100 MeV/c^2 of the world average J/ψ mass of 3096.9 MeV/c^2 . Approximately 80,000 J/ψ are reconstructed with very good signal to background ratio ($\sim$10) at the peak region.

B mesons are reconstructed by combining J/ψ candidates and other charged tracks. B meson masses and decay lengths are calculated by fitting the tracks to a common secondary vertex, constraining the two muon invariant mass to be the J/ψ mass, and constraining the B meson momentum to the primary vertex. A χ^2 confidence level of 1% for the vertex constrained fit is required for all decay modes. $B_u^\pm$, B_d^o and B_s^o mesons are reconstructed for the mass measurements. The p_t scale is calibrated using the J/ψ peak, and dE/dX loss due to detector material is corrected for using a detailed study of photon conversions.

For the $B_u^\pm$ meson mass measurement we used the decay mode $B_u^\pm \rightarrow J/\psi\ K^\pm$. To reduce the large background at lower p_t , a tight p_t requirement of 2 GeV/c is applied to the kaon. In addition, to enrich the B fraction for the J/ψ candidates, a p_t cut of 8 GeV/c is applied to the B system. To further reduce background we require $c\tau$, the proper decay length of the B system, to be $\geq 100 \mu m$. The invariant mass spectrum is shown in upper plot in the figure 1. There are about 147 signal events in the peak region. The invariant mass and error were extracted using an unbinned likelihood fit assuming a Gaussian signal on a linear background. The fit gives $5279.1 \pm 1.7 \pm 1.4 MeV/c^2$, where the first error is statistical and the second is systematic.

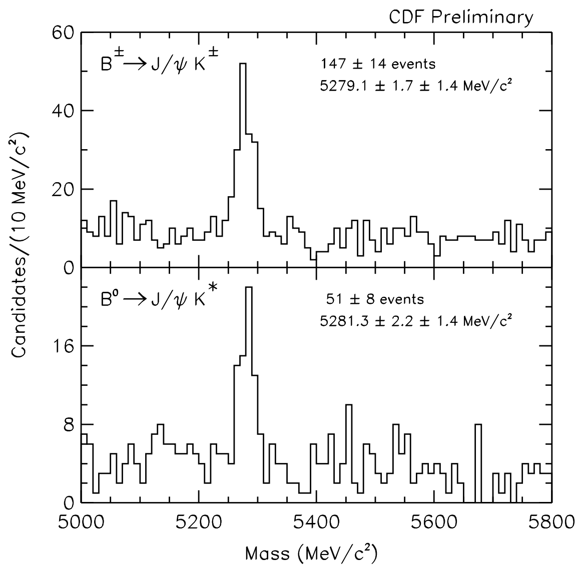

Figure 1: $B^\pm \rightarrow J/\psi\ K^\pm$ (top) and $B^0 \rightarrow J/\psi\ K^{*0}$ (bottom) invariant mass distribution

For the B_d^o meson mass measurement we used the decay mode $B_d^o \rightarrow J/\psi\ K^{*o}(892)$. The $K^{*o}(892)$ candidates are selected with invariant mass within a 50 MeV/c^2 window of the $K^{*o}(892)$ mass for a two track combination of oppositely charged tracks assumed to be a kaon and a pion. To reduce combinatoric backgrounds, we require the p_t of the $K^{*o}(892)$ candidates to be greater than 3 GeV/c , $p_t(B)\geq 8$ GeV/c and $c\tau \geq 100$ μm . The resulting mass distribution was fit with a Gaussian peak and a linear background shape. There are about 51 signal events in the peak region and the fit mass is $5281.3 \pm 2.2 \pm 1.4 MeV/c^2$, as shown in lower plot in figure 1.

For the B_s^o meson mass measurement we used the decay mode $B_s^o \rightarrow J/\psi\ \phi$. The ϕ candidates are selected with invariant mass within $10 MeV/c^2$ of the ϕ mass for a two track combination of oppositely charged tracks assuming they are kaons. Additional cuts are $p_t(\phi) \geq 2$ GeV/c , $p_t(B) \geq 6$ GeV/c and $c\tau \geq 0$. The resulting mass distribution was fit with a Gaussian peak and a linear background shape. In figure 2 there are 32 signal events in the peak region and the fit mass is $5369.9 \pm 2.3 \pm 1.3 MeV/c^2$

The above mass measurement results are tabulated with the current CLEO and LEP average results [4] in table 1. The CDF results are consistent with CLEO and LEP results and are comparable in uncertainties.

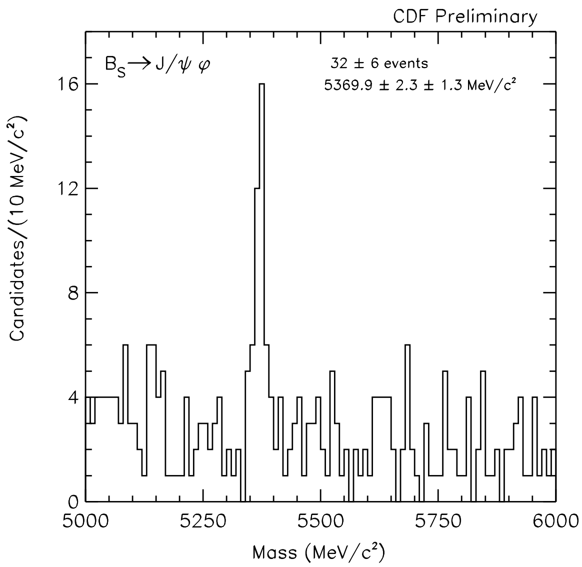

Figure 2: $B_s^0 \rightarrow J/\psi\varphi$ invariant mass distribution

Table 1: Summary of the CDF results on B meson masses compared with other experiments.

B mesons	CDF MeV/c^2	MeV/c^2
$B_u^{\pm}$	5279.1±1.7±1.4	5278.7±2.0 (CLEO)
B_d^0	5281.9±2.2±1.4	5279.0±2.0 (CLEO)
B_s^0	5369.9±2.3±1.3	5368.5±5.3 (LEP ave.)

3 B Meson Lifetime Measurements

Measurement of the lifetimes for various b-flavored hadrons provides a way to understand the non-spectator mechanism. The theoretical predictions on the lifetime difference between charged and neutral B mesons are only about ~5% [5] while that of the D mesons are measured to be more than a factor of 2. It is very important to have measurement sensitivity better than the predicted difference to study details of the decay mechanism.

For the lifetime measurement, very accurate primary vertex position measurement is crucial. In CDF the beam position in the transverse plane is very small (35 μm in both x and y axis) and the position was monitored from run to run. The transverse plane is the plane perpendicular to the beam axis. For the inclusive lifetime study only 1A data are used, while for the exclusive lifetime study we also include run 1B data and the total integrated luminosity for this analysis is 68 pb^{-1} .

3.1 Exclusive $B_{u,d}$ Lifetime Measurements

The J/ψ selection and B meson reconstruction for the exclusive lifetime analysis is quite similar to the B meson mass analysis. However there are some differences in the analysis cuts to optimize the lifetime measurement. The $c\tau$ cut is removed for this analysis, and no vertex pointing constraint is applied in the vertex fit to avoid bias. Also, kinematic cuts are optimized for the analysis.

The B decay modes used in this analysis are $B \rightarrow \Psi^X K^X$ where Ψ^X stands for a J/ψ or ψ' and K^X stands for $K^{\pm}$, K_S^o , or $K^*(892)$. To have a good vertex resolution, SVX hits are required for both of the muon tracks. A total of 140,000 J/ψ 's were selected for the analysis.

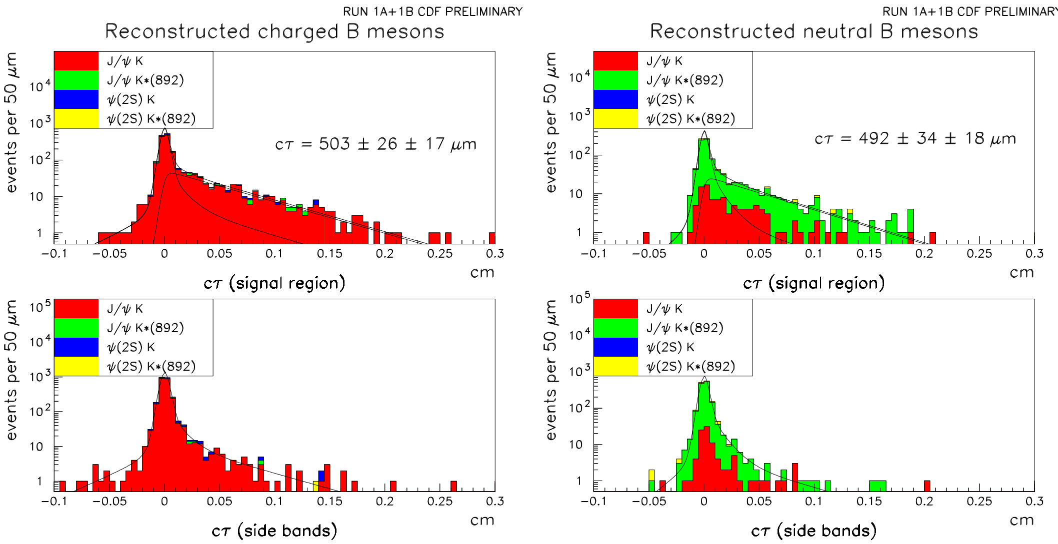

Figure 3: Signal and sideband $c\tau$ distributions for B^+ (left) and B^0 (right).

Table 2: B_u^+, B_d^0 lifetimes and their ratio for exclusive and inclusive methods.

psec.	$\tau(B_u^+)$ psec.	$\tau(B_d^0)$ psec.	τ^+/τ^0
$\Psi^X K^X$	1.68±0.09±0.06	1.64±0.11±0.06	1.02±0.09±0.01
$D^{(*)}l$	1.51±0.12±0.08	1.57±0.08±0.07	0.96±0.10±0.05
combined			1.00 ± 0.07

The decay length in the transverse plane, L_{xy} , is defined to be the projected distance between the primary vertex and the secondary(B) vertex position to the transverse direction of the B.

$$L_{xy} \;=\; \frac{(\vec{V}_{sec} - \vec{V}_{prim}) \cdot \vec{P}_t(B)}{\vec{P}_t(B)} \tag{1}$$

The proper decay length, $c\tau$, is then derived as follows:

$$c\tau \;=\; L_{xy}\frac{M(B)}{P_t(B)}, \tag{2}$$

where $M(B)$ is the mass and the $p_t(B)$ is the transverse momentum of the B meson.

B meson candidates are selected by requiring the mass difference, $|\Delta M|$, to be less than 30 MeV/c^2 with respect to the world average of the B meson mass. The $c\tau$ distributions for charged and neutral B mesons are shown in the figure 3. The background shape is determined by fitting the side band region, 60 $MeV/c^2 \leq |\Delta M| \leq$120 MeV/c^2 , with a Gaussian peak and an exponential tail. The shape of the signal region is assumed to be a sum of the sideband shape and an exponential shape smeared with resolution. Results of the unbinned fit including event by event resolution variation are shown in table 2. Since much of the systematic error, which comprises misalignment, trigger bias and beam stability, is common for the charged and neutral B meson analysis, the ratio of the lifetimes has a much smaller systematic error.

3.2 Inclusive $\mathbf{B}_{u,d}$ Lifetime Measurements

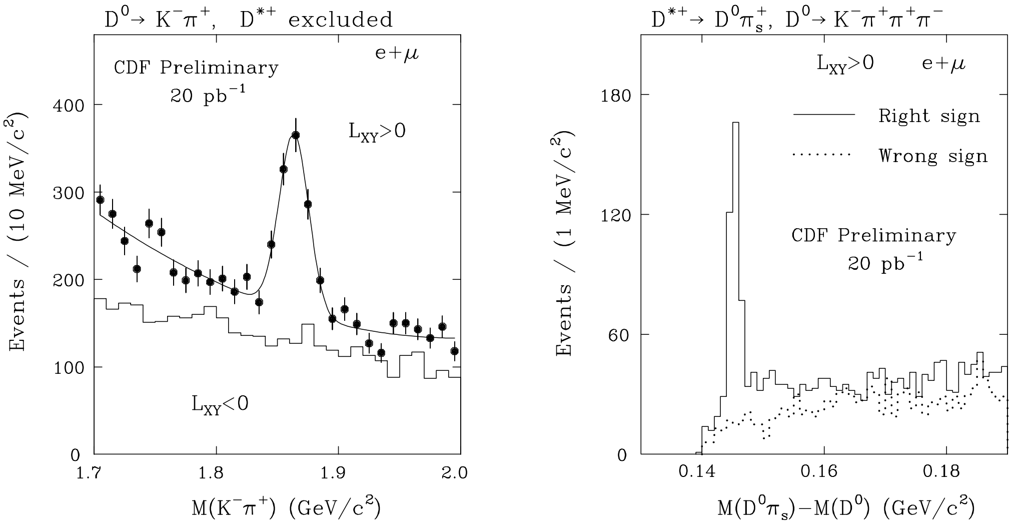

Figure 4: D, D^* invariant mass peaks used in the semi-exclusive B lifetime analysis. Left: $D^0 \to K^-\pi^+$, right: $D^{*+} \to D^0\pi^+, D^0 \to K^-\pi^+$

In this method, we reconstructed charmed mesons from the semileptonic decays of B mesons using a large sample from the inclusive electron and muon triggers. The charmed mesons are reconstructed with tracks which are in a cone around the trigger electrons or muons. The following and corresponding charge conjugate modes are used in the analysis.

I. $D^o \to K^- \ \pi^+$
II. $D^{*+} \to D^o \ \pi^+$, $D^o \to K^- \ \pi^+$
III. $D^{*+} \to D^o \ \pi^+$, $D^o \to K^- \ \pi^+$ X
IV. $D^{*+} \to D^o \ \pi^+$, $D^o \to K^- \ \pi^+ \ \pi^+ \ \pi^-$

Mode III is dominated by $D^o \to K^-\rho^+$ decays. Four plots of the decay modes are shown in figures 4 and 5. Clean signals of charmed meson are seen in all of the plots. The distributions show no hint of peaks from wrong sign charge combinations between the charmed meson and the lepton.

The decay length in the transverse plane, L_{xy} , is defined to be the projected distance between the primary vertex position and the reconstructed B vertex position to the transverse direction of B^X. Here B^X is the partial reconstruction of a B meson with a lepton and a charmed meson.

Then $c\tau$ is defined as follows:

$$c\tau \ = \ L_{xy} \cdot \frac{M_B}{p_t(B^X)} \cdot K \tag{3}$$

where K is the average correction factor estimated from Monte Carlo study. For channel I, the D's which form D^* when combined with a pion are specifically excluded to reduce confusion of the charge of the originating B meson, hence purifying the charged B mesons. The rest of the channels, II, III and IV, are from the neutral B mesons. Because of D^{**} production, the non-resonant part of charged π production, and the inefficiency in excluding the D^* component from channel I, there is some cross talk in identifying the charge of the B meson. The relative fractions of neutral and charged B mesons in all the decay channels are estimated through extensive Monte Carlo study. The uncertainties of the sample composition are estimated

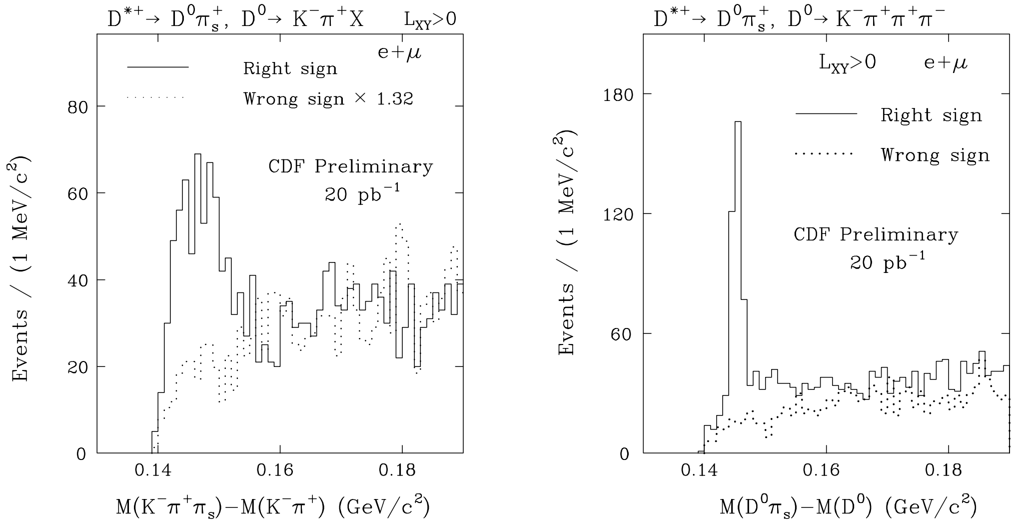

Figure 5: D^* invariant mass peaks used in the semi-exclusive B lifetime analysis. Left: $D^{*+} \to D^0\pi^+, D^0 \to K^-\pi^+X$, right: $D^{*+} \to D^0\pi^+, D^0 \to K^-\pi^+\pi^+\pi^-$

to have negligible effect in the lifetime measurement. The final results of the measurements are shown in table 2. In figure 6 we show the measurements of the charged to neutral $B_{u,d}$ lifetime ratio at LEP and at CDF. CDF results are consistent to the LEP results[6].

3.3 B_s^o Lifetime Measurement

The lifetime of the B_s^o meson is measured[7] using two methods. First, the fully reconstructed $B_s^o \to J/\psi\ \phi$ decay channel is used. The analysis technique is similar to the $B_{u,d}$ meson lifetime measurement. Eight events after background subtraction are used in the fit to determine a lifetime of $\tau = 1.74^{+1.08}_{-0.69} \pm 0.07$psec. The fit result shows a very large statistical error compared to the systematic error. With more statistics from 1B data, we expect a much improved measurement in a short time.

Secondly, B_s^o mesons are partially reconstructed for the decay channel $B_s^o \to D_S l\nu$, $D_S \to \phi\pi$. About 76 correct sign D^* are found in this channel for the B_s^o lifetime determination. The result of the fit is $\tau = 1.42^{+0.27}_{-0.23} \pm 0.11$ psec. The error is dominated by the statistical uncertainty.

4 Rare B Decays

In the Standard Model of electroweak interactions, rare decays of B mesons involving flavour changing neutral currents are forbidden at the tree level and proceed only through higher order processes. Deviation from the predicted branching ratios could indicate new physics beyond the Standard model. The large number of B enriched dimuon triggers enables CDF to compete with other experiments in the search of these decays.

We have searched for $B \to \mu\mu K$, $B \to \mu\mu K^*$ and $B \to \mu\mu$, where $\mu\mu$ pairs are not coming from J/ψ or ψ' decay. For the $\mu\mu K$ and $\mu\mu K^*$ channel, the selection criteria of the final sample are quite similar to those of the mass measurement analysis. The major difference is that the $\mu\mu$ pairs from the resonances J/ψ and ψ' are specifically excluded for the final selection. The kinematic cuts and $c\tau$ cuts are optimized and an isolation cut is applied to the B meson candidate to achieve the best limit. Then the ratio between the resonant and non-resonant production of $\mu\mu$ pairs in the B mass region is measured. The measurement of the ratio ensures the cancellation of much of the common systematic error. The 90 % confidence level limits are shown in the table 3, along with the CLEO measurements[8] and Standard model predictions [9].

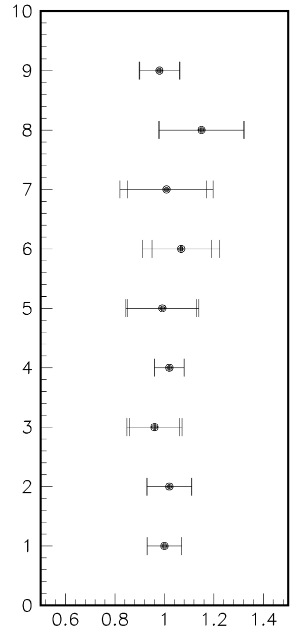

Figure 6: World B^+/B^0 lifetime ratios.

Table 3: 90% C.L. limits for the non-resonant $B_u \to \mu\mu K^{\pm}$,$B_d \to \mu\mu K^*$ $B_d \to \mu\mu$ and $B_s \to \mu\mu$ branching ratios compared to Standard Model predictions and recent CLEO measurements.

	BR($B_u \to \mu\mu K^{\pm}$)	BR($B_d \to \mu\mu K^*$)	BR($B_d \to \mu\mu$)	BR($B_s \to \mu\mu$)
CDF	1.0×10^{-5}	2.5×10^{-5}	1.6×10^{-6}	8.4×10^{-6}
CLEO	0.9×10^{-5}	3.1×10^{-5}	5.9×10^{-6}	
S.M.	4.4×10^{-7}	2.3×10^{-6}	8.0×10^{-11}	1.8×10^{-9}

For the $\mu\mu$ channel, we estimated the $B_d^o \to \mu^+\mu^-$ and $B_s^o \to \mu^+\mu^-$ events from the invariant mass distributions of $\mu\mu$ which fell into the window of $\pm$ 75 MeV/c^2 around the measured masses of B mesons. Other cuts are very similar to the $\mu\mu K^{\pm}$, $\mu\mu K^*$ channels. The limits are shown in table 3. This analysis is the first to set a limit on production of $B_s^o \to \mu^+\mu^-$, and the $B_d^o \to \mu^+\mu^-$ result is a significant improvement over the CLEO limit.

5 $B^o\bar{B}^o$ Mixing

Mixing between the B^o and $\bar{B}^o$ occurs when one of the B changes to the other. This phenomenon occurs when the mass difference between the two weak interaction eigenstates is very small. The formalism which describes the B^o - $\bar{B}^o$ mixing is very similar to that of K_S^o - $\bar{K}_S^o$ mixing. If a pure B^o state is produced at time t=0, then at later time it will evolve into a new state which contains a mixture of B^o and $\bar{B}^o$. The probability that the state will change to $\bar{B}^o$ at time t is given by

$$P(B^o(0) \to \bar{B}^o(t)) \;=\; 0.5 \cdot exp(-t/\tau)[1 - cos(\Delta m t)] \tag{4}$$

where τ is the lifetime of the B meson and Δm is the mass difference between the two B eigenstates. For convenience, we define $x = \Delta m/\Gamma$, where Γ is the average width of the eigenstates and obtain a formula for time the integrated mixing probability:

$$P(B^o \to \bar{B}^o) = \chi = \frac{x^2}{2(1+x^2)} \tag{5}$$

The mixing parameters $x_{d,s}$ for the $B^o_{d,s}$ mesons have strong correlations with CMK matrix elements, $V_{t,(d,s)}$. Note that χ approaches one at large x. When the mixing is very large, the χ measurement is a very insensitive method to determine x.

The inclusive χ measurement has two components, namely χ_d for B^o_d mixing and χ_s for B^o_s mixing. The average of the parameters is $\bar{\chi} = F_d\chi_d + F_s\chi_s$, where the F_d and F_s are the relative production ratios of B^o_d and B^o_s . The direct measurement of x_d is performed in CDF through time dependent oscillation measurement.

5.1 Time Integrated Mixing Measurement

When $b\bar{b}$ quark pairs are produced, the flavour of one b quark reveals the flavour of the other when mixing does not occur. The flavour of a b quark which decays semileptonically could be found from $b \to l^- + c$ and $\bar{b} \to l^+ + \bar{c}$. We studied two channels for this analysis using $e\mu$ and $\mu\mu$ triggers. The ratio, R, of the number of events with like-sign leptons (LS) to the number of opposite-sign (OS) leptons are defined by:

$$R = \frac{LS}{OS} = \frac{2\bar{\chi}(1-\bar{\chi})}{\bar{\chi}^2 + (1-\bar{\chi})^2} \tag{6}$$

5.2 $\bar{\chi}$ Analysis with $e\mu$ Data

Some fraction of the leptons come from the sequential decays, $b \to c \to l^+$. Also, fake lepton contributions are estimated.

$$R = \left(\frac{LS}{OS}\right)_{exp} \frac{(1-F_{e\mu}(LS))}{(1-F_{e\mu}(OS))} = \left(\frac{2\bar{\chi}(1-\bar{\chi}) + [\bar{\chi}^2 + (1-\bar{\chi})^2]f_s}{\bar{\chi}^2 + (1-\bar{\chi})^2 + 2\bar{\chi}(1-\bar{\chi})f_s + f_c}\right) \tag{7}$$

where

- $f_s = \#(b \to c \to l)/\#(b \to l)$ is the sequential decay fraction which is estimated via Monte Carlo studies to be 0.136$\pm$0.023.
- $f_c = \#(c\bar{c})/\#(b\bar{b})$ is the charm fraction from $c\bar{c}$ production in the sample. By fitting P_t^{rel} distributions of Monte Carlo data we estimate $f_c = 0.007 \pm 0.011$.
- $F_{e\mu}(LS)$ = fraction of fake leptons in the LS sample and $F_{e\mu}(OS)$ = fraction of fake leptons in the OS sample. These quantities are estimated by releasing lepton identification cuts. The estimations are $F_{e\mu}(LS) = 0.396 \pm 0.031$ and $F_{e\mu}(OS) = 0.255 \pm 0.021$.

We observe 1710 opposite-sign and 861 like-sign $e\mu$ events. Using the formula we obtain:

$$\bar{\chi} = 0.130 \pm 0.010 \pm 0.009$$

where the first error is statistical and the second is systematic. The major contributions to the systematic errors are uncertainty on the sequential fraction and the fake lepton fraction, $F_{e\mu}$. The result is plotted in the figure 7, assuming a B_d fraction F_d=0.391 and a B_s fraction F_s=0.117. The measurement provides the bound in the $\chi_d - \chi_s$ plane as shown. Also shown are the ARGUS[10] and CLEO[11] results in the region. The shaded area is allowed by the Standard Model.

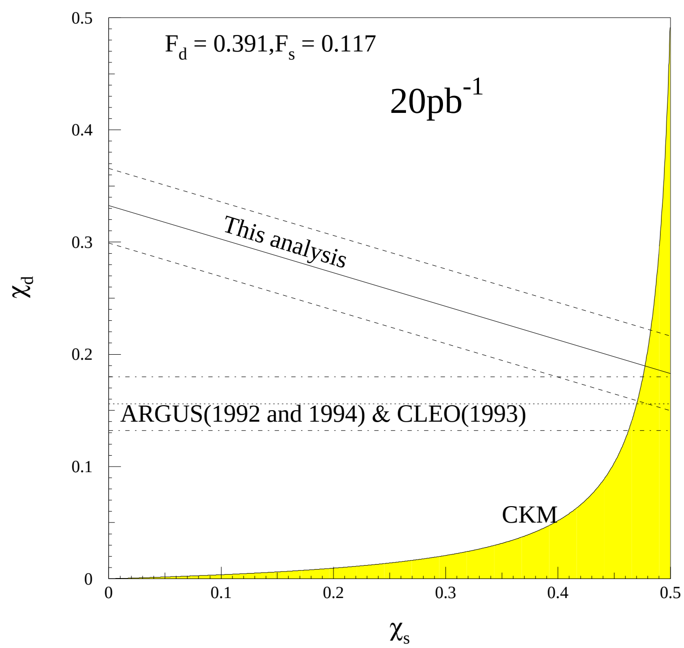

Figure 7: The mixing parameter for B_d versus that for B_s. The bands represent 1σ uncertainty

5.3 $\bar{\chi}$ Analysis with $\mu\mu$ Data

For the $\mu\mu$ channel, a similar technique is applied to estimate $\bar{\chi}$. However, the $b\bar{b}$ fractions of LS and OS are estimated directly from the fits to the impact parameter distributions of the muons. This method exploits the fact that the impact parameter distributions of muons are different from the backgrounds. Muons from B decay have non-zero impact parameters because of the displaced vertex of the B decay, while background tracks are mainly from the primary vertex and impact parameter distributions are peaked at the zero. Two dimensional likelihood fits were made to the distributions with template histograms for the distributions of signal and background to extract the B fraction. We obtain 882 ± 55 for like-sign and 1804 ± 103 for opposite-sign from the likelihood fit. From this we estimate:

$$\bar{\chi} \ = \ 0.118 \ \pm \ 0.021 \ \pm \ 0.026$$

where the systematic errors are dominated by the uncertainty of the sequential decay fraction. In figure 8 we show both of the CDF $\bar{\chi}$ measurements with LEP results[12]. CDF results are consistent with other measurements.

5.4 Time Evolution $B^o\bar{B}^o$ Mixing Measurement

A half million low p_t dimuon triggers are used for the time dependent mixing parameter measurement. To reduce background from double semileptonic decays from the same B, we require the dimuon invariant mass to be greater than 5 GeV/c^2 . After tight μ selection criteria, we are left with ~100,000 events. We further reduced the sample by applying a secondary vertex tagging algorithm which selects events with one of the muons forming a good displaced vertex with at least two other tracks nearby. The tracks which are used in vertex fit (excluding the μ) are required to be consistent with the decay products of D's, which we call D^X. Substantial backgrounds from sequential decays are rejected by requiring p_t^{rel}, the transverse momentum of the μ in the direction of D^X, to be greater than 1.3 GeV/c .

The L_{xy} and proper decay length are measured the same way as in the inclusive lifetime analysis. The kinematic correction factor, K, was estimated from Monte Carlo study. After all the cuts, the sample was

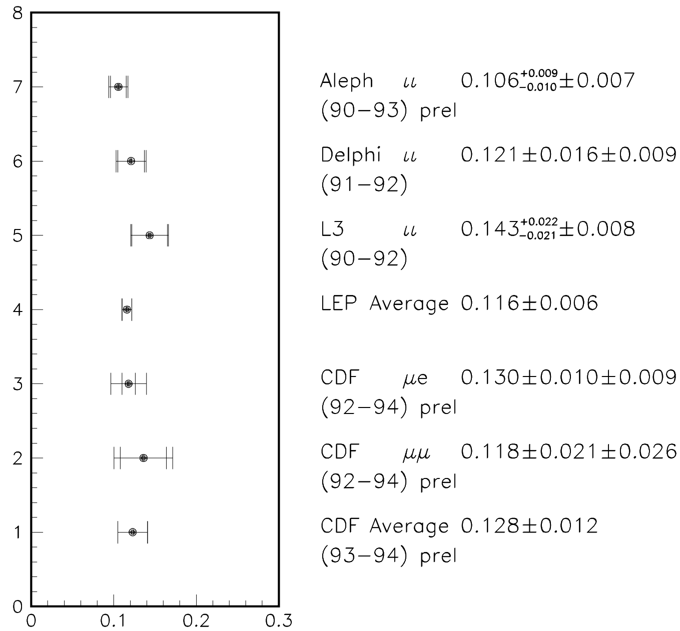

Figure 8: Comparison of the current measurements of $\bar{\chi}$ at Fermilab and LEP.

reduced to 1516 like-sign and 2357 opposite-sign events. In figure 9 the like-sign fraction is plotted as a function of pseudo $c\tau$. An oscillatory behavior is evident in the figure. The fake muon fraction is estimated to be 10$\pm$3.5% by an impact parameter fit on the muons. The $c\bar{c}$ contribution in our sample is estimated to be $\sim$1%. The sequential decay fraction is estimated by a 3 component fitting of p_t^{rel} with three distribution shapes: muons from direct b, sequential decay and $c\bar{c}$.

A fit was made to the like-sign fraction to estimate Δm_d. A mixing parameter value for the B_s $\bar{\chi}_s = 0.5$ was used as an input parameter. The fraction of B_d^o and B_s^o in our sample are 0.37$\pm$0.03 and 0.15$\pm$0.04, respectively, and the result of the fit is

$$\Delta m_d = 0.44 \pm 0.12 \pm 0.14 \text{psec.}^{-1}$$

The systematic error is dominated by the uncertainty in the sequential fraction. We expect a considerable reduction of the errors with the improved statistics using run 1B data.

6 Polarization Measurements of B Mesons

In this section, we describe measurements of the longitudinal polarization fractions Γ_L/Γ in the Pseudoscalar-to-Vector-Vector decays $B_d \to J/\psi K^{*0}$ and $B_s \to J/\psi\phi$. Measuring the polarization in the decay $B_d \to J/\psi K^{*0}$ was inspired by its potential use in CP violation studies in e^+e^- colliders [13]. In addition, a measurement of Γ_L/Γ can be used to test theoretical predictions which depend on the factorization hypothesis [14].

The decay distribution for $B_d \to J/\psi K^{*0}$, $J/\psi \to \mu^+\mu^-$, $K^{*0} \to K^+\pi^-$ can be written as [15]:

$$\frac{d^2\Gamma}{d\cos\theta_{K^*}d\cos\theta_\psi} \quad \propto \quad \frac{1}{4}\sin^2\theta_{K^*}(1+\cos^2\theta_\psi)\frac{\Gamma_T}{\Gamma} + \cos^2\theta_{K^*}\sin^2\theta_\psi\frac{\Gamma_L}{\Gamma}$$

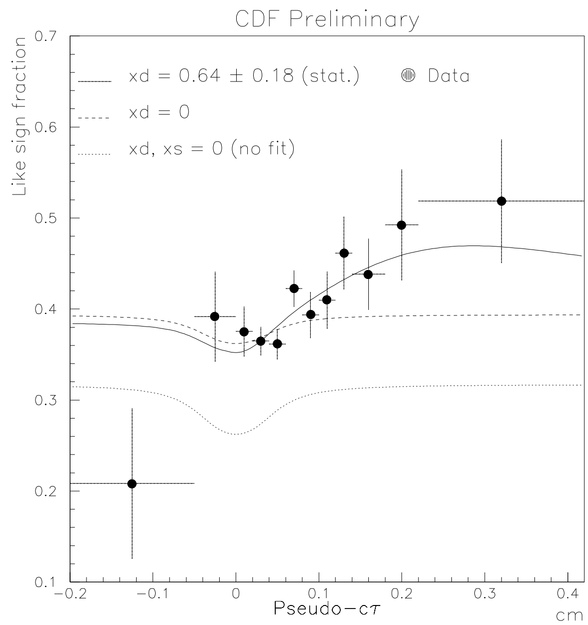

Figure 9: Like-sign fraction versus $c\tau$. The solid line is our fit to the data; the dashed line is our fit after forcing x_d=0 and the dotted line is a prediction assuming just the sequential decay contribution and both x_d and $x_s = 0$

Table 4: Γ_L/Γ measurements

mode	$B_d \to J/\psi K^{*0}$	$B_s \to J/\psi\phi$
ARGUS	$0.97 \pm 0.16 \pm\ 0.15$	-
CLEO	$0.80 \pm 0.08 \pm\ 0.05$	-
CDF	$0.65 \pm 0.10 \pm 0.04$	$0.56 \pm 0.21\,^{+0.02}_{-0.04}$
World Average	0.74 ± 0.07	-

where the helicity angle θ_{K^*} is the decay angle of the kaon in the K^{*0} rest frame with respect to the K^{*0} direction in the B rest frame. Similarly, θ_ψ is the decay angle of the muon in the J/ψ rest frame with respect to the J/ψ direction in the B rest frame.

Event selection and reconstruction for the decay $B_d \to J/\psi K^{*0}$ is very similar to that of B mass measurement. We observe a signal of 65 ± 10 events above a background of $\sim$14. The background distribution is taken to be unpolarized as determined from a fit to events in the sidebands around the B_d mass. The fit results for longitudinal polarization fraction for $B_d \to J/\psi K^{*0}$ decay are shown in table 4. The lower value of Γ_L/Γ compared to the ARGUS[16] and CLEO[17] results, suggests that the $B_d \to J/\psi K^{*0}$ decay mode may be more difficult to use for CP violation studies than previously believed.

For the decay $B_s \to J/\psi\phi$, a signal of 19 ± 5 events is above a background of $\sim$2. The fit results are shown in the table 4. This is the first measurement of the longitudinal polarization fraction for this decay.

Table 5: Expected number of B's in specific decays channels in run 1B and II.

	Run 1A 20 pb^{-1}	1A+1B 120 pb^{-1}	Run II 2 fb^{-1}
$B \rightarrow J/\Psi K^{\pm}$	175	~1050	~70,000
$B \rightarrow J/\Psi K^{*0}$	95	~570	~40,000
$B \rightarrow J/\Psi K^0_S$	51	~306	~20,000
$B \rightarrow J/\Psi \varphi$	33	~198	~12,000
$B_{u,d} \rightarrow l D_0^{*+}$	~ 1,500	~ ~9,000	~10^5
$B_s \rightarrow l D_s$	76	~456	~10^5

7 Prospects for B physics at CDF

We expect to collect ~100 pb^{-1} of data by the end of the run 1B. Combining this with existing 1A data we will have ~120 pb^{-1} in the near future. The Tevatron upgrade with the Main Injector will deliver ~1 fb^{-1} per year after RUN II starts. In parallel with the accelerator upgrade, many detector upgrade projects are underway in order to cope with the high luminosity environment. These include new tracking chambers, plug calorimeters and trigger systems. It is reasonable to expect to collect ~2 fb^{-1} of data from RUN II. In table 5 we make a simple extrapolation to show the B reconstruction capability in each stage. More than 2000 fully reconstructed B's and ~10,000 partially reconstructed B's which decay semileptonically will be available after RUN 1B.

The most important goal of the CDF B physics program in RUN II is to observe CP violation in the B system. CP violating asymmetry occurs through interference in the $B^o \bar{B}^o$ mixing. The asymmetry is defined as

$$A = \frac{\Gamma(B \rightarrow f) - \Gamma(\bar{B} \rightarrow \bar{f})}{\Gamma(B \rightarrow f) + \Gamma(\bar{B} \rightarrow \bar{f})} \tag{8}$$

where f is the final decay product. The most clean signal occurs when $f = \bar{f}$ (for example, $B_o \rightarrow J/\Psi\ K_s^o$), so the flavour of the parent B must be tagged.

In CDF, several studies of B flavour tagging methods are in progress. The lepton tagging method uses the charge of the lepton from the other B decay to identify flavour. The jet charge tagging method estimates jet charge of the away side jet from the other B decay. Jet charge is defined as a momentum weighted average of the charges of the tracks in a cone around a jet. Due to the leading particle effect, the jet charge is correlated with the charge of the originating b quark. The same side tagging method exploits the charge correlation effect between a B and a charged track when they are produced at the same time. This includes both B^{**} production and nonresonant $B\pi$ production at small Q values. LEP measurements [18, 19] show a substantial fraction, ~20-30%, of B is from B^{**}, which decays to $B\pi$.

For the asymmetry measurement, the most frequently used quantity which describes the effectiveness of the flavour tagging is ϵD^2 , the 'effective tagging efficiency'. Here ϵ is the applicability of the method and D is the dilution factor which describe the correctness of the tagging. D is defined as $(N_{right} - N_{wrong})/(N_{right} + N_{wrong})$

We estimate ϵD^2 directly from data for both of the soft muon tagging and jet charge tagging:

- Soft μ tag method:
  $\longrightarrow\ \epsilon D^2 = 0.0096\ ^{+0.0022}_{-0.0031}$
- Jet Charge method:
  $\longrightarrow\ \epsilon D^2 = 0.0101 \pm 0.0033 \pm 0.0021$

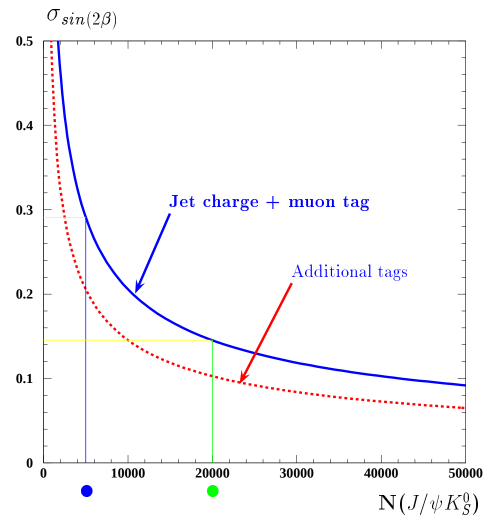

Figure 10: Estimate of CDF $sin(2\beta)$ resolution for two luminosity and flavour tagging efficiencies.

7.1 Prospect for $sin(2\beta)$ Measurement

High trigger efficiency for the $B \to J/\psi + X$ decay at CDF will put us on a unique position in the asymmetry study on the B decay modes which include J/ψ . For example, β, one of the three CP violation parameters, could be determined through tagged asymmetry measurement in the decay of $B \to \psi K_S^0$. The sensitivity of the asymmetry measurement can be expressed as:

$$\sigma_{sin(2\beta)} = \frac{1}{(\sqrt{\epsilon}D)\sqrt{N_{B\to\psi K_S^0}} \cdot \frac{x_d}{1+x_d^2}\sqrt{\frac{S}{S+B}}} \tag{9}$$

where S and B are the amount of the signal and background in the sample.

In figure 10 we plot the error of $sin(2\beta)$ versus the number of J/ψ K_S^o events. The upper curve shows the sensitivity with the two tagging methods described above. The lower curve assumes the four times larger ϵD^2 with improved and additional tagging methods, including same side tagging and soft electron tagging. Two dots are shown in the plot. For the lower point, the simple extrapolation of the number of J/ψ K_S^o events from 1A data is made to estimate the error with the RUN II luminosity ($\sim$2fb^{-1}). For the higher point, we assume acceptance improvements for the leptons by increasing η coverage from 1 to 2 and lowering the dimuon trigger threshold to $p_t \geq 1.5$ GeV/c . With these improvements, a measurement accuracy of 0.08 for $sin(2\beta)$ is achievable with the expected luminosity.

7.2 Prospect for $sin(2\alpha)$ Measurement

The parameter $sin(2\alpha)$ could be measured via the decay mode $B^0 \to \pi^+\pi^-$. A sophisticate displaced vertex finding trigger processor, which has impact parameter resolution of 25 μm , is under study. This would enable CDF to select non-leptonic decays of $b\bar{b}$ events efficiently by tagging secondary vertices. We expect $\sim$5 events of this decay mode per pb^{-1} . Extraction of the $\pi^+\pi^-$ decay mode from the modes which includes kaons could be achieved by the invariant mass separation. A few particle identification techniques are being considered to help in extracting the $\pi^+\pi^-$ signal. Figure 11 displays the expected mass distribution for the combination of the four decay channels when both of the tracks are assigned with pion masses assuming

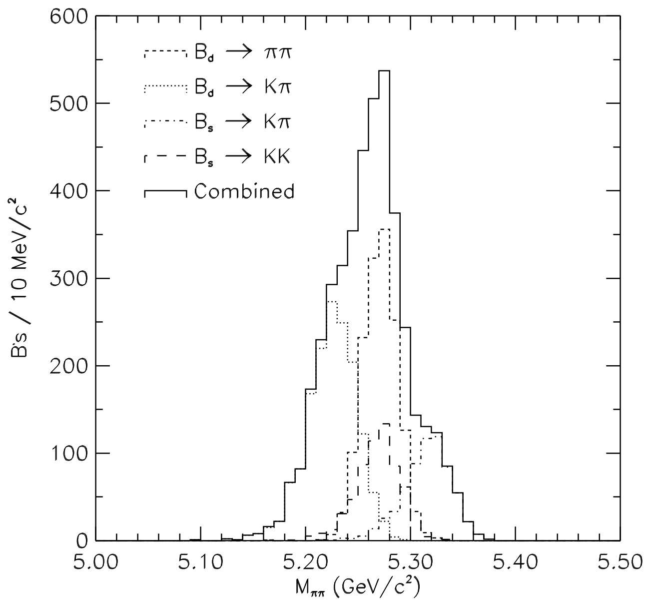

Figure 11: Expected mass distribution for the combination $B^o \to \pi^+\pi^-$, $B_d \to K\pi$, $B_s \to K\pi$

existing tracking chamber resolutions. At $p_t(B)$ $\sim$6 GeV/c the mass resolution σ_m $\sim$28 MeV/c^2 . With these assumptions, we expect a measurement accuracy of 0.08 for $sin(2\alpha)$.

7.3 Prospect for CP Asymmetry in $B_s \to J/\psi\phi$

The CP asymmetry in $B_s \to J/\psi\phi$ measures the weak phase of the CKM matrix element V_{ts}. We expect $\sim$12,000 events for this decay in Run II. With kaon identification by the time-of-flight system, the total flavor tagging efficiency would be improved to 11%. B_s oscillation would modulate the CP asymmetry. The finite resolution will smear the oscillations and result in additional dilution. Neglecting this effect we can expect a precision on the asymmetry of $\pm$0.09.

8 Conclusions

In the last few years, CDF has produced high quality results in B physics. By including the large Run 1B data sample, CDF will significantly improve the B spectroscopy, lifetime and mixing measurements. With the expected integrated luminosity of Run II, observation of CP violation is within reach.

References

[1] K. Byrum, "Charmonium Production, B Quark and B Meson Production and $b\bar{b}$ Correlations at CDF", Proceedings of the XXVII Int. Conf. on High Energy Physics, p. 989, Glasgow, UK, July 1994.

[2] F. Abe *et al.*, Nucl. Instr. Meth. Phys. Res. **A 271**, 387 (1988); F. Bedeschi *et al.*, Nucl. Instr. Meth. Phys. Res. **A268**, 50 (1988); G. Ascoli *et al.*, Nucl. Instr. Meth. Phys. Res. **A268**, 33 (1988).

[3] D. Amidei *et al.*, Nucl. Instr. Meth. Phys. Res. **A350**, 73 (1994).

[4] V. Canale, "Exclusive B-hadron Lifetimes and Masses at LEP", Proceedings of the "XXXth Recontres de Moriond", QCD and High Energy Hadronic Interactions, Les Arcs, Savoie, France, March 19-26, 1995.

[5] I. Bigi, preprint UND-HEP-95-BIG06; tp appear in Proceedings of the 6th International Symposium on Heavy Flavour Physics, Pisa, Italy, June, 6-10,1995.

[6] Giuliana Rizzo, "b Hadron Lifetimes at LEP", Talk given at the 3rd International Workshop on B-Physics at Hadron Machines, Oxford, UK, 10-14 July, 1995.

[7] F. Abe *et al.*, "Measurement of the B_s Meson Lifetime", FERMILAB-PUB-94/420-E, submitted to Phys. Rev. Lett.

[8] R. Ammar *et al.*, Phys. Rev. D **49**, 5701 (1994).

[9] A. Ali, "Rare Decays of B Mesons", DESY 91-080 (1991), Proceedings of the First Int. A. D. Sakharov Conf. on Physics, Lebedev Physics Inst., Moscow, USSR (1991).

[10] H. Albrecht *et al.*, Z. Phys. **C55**, 357 (1992) H. Albrecht *et al.*, Phys. Lett. **B324**, 249 (1994),

[11] J. Bartlett *et al.*, Phys. Rev. Lett. **71**, 1683 (1993).

[12] Achille Stocchi, "$B^o(t) - \bar{B}^o(t)$ Oscillations at LEP", Talk given at the 3rd International Workshop on B-Physics at Hadron Machines, Oxford, UK, 10-14 July, 1995.

[13] I. Dunietz *et al.*, Phys. Rev. D **43**, 2193 (1991).

[14] M. Bauer, B. Stech, and M. Wirbel, Z. Phys. C **34**, 103 (1987); M. Wirbel, B. Stech, and M. Bauer, Z. Phys. C **29**, 637, (1985).

[15] G. Kramer and W.F. Palmer, Phys. Rev. D **46**, 2969 (1992), G. Kramer and W.F. Palmer, Phys. Lett. **B279**, 181 (1992).

[16] H. Albrecht *et al.*, Phys. Lett. B **340**, 217 (1994).

[17] M.S. Alam *et al.*, Phys. Rev. D **50**, 43 (1994).

[18] S. Schael (ALEPH Coll.), "Excited Beauty at LEP", Proceedings of the "XXXth Recontres de Moriond", QCD and High Energy Hadronic Interactions, Les Arcs, Savoie, France, March 19-26, 1995.

[19] C. Shepherd-Themistocleous (OPAL Coll.), "$B - \pi$ Flavour-Charge Correlations and Evidence for B^{**} and B_s^{**}", Proceedings of the "XXXth Recontres de Moriond", QCD and High Energy Hadronic Interactions, Les Arcs, Savoie, France, March 19-26, 1995.